Cobalt(II) Substituted Derivatives of Carcinus maenas Hemocyanin: Magnetic Characterization, Magnetooptic, and Kinetic Studies Regarding the Geometry of the Active Site

ARTICLE *in* INORGANIC CHEMISTRY · DECEMBER 1996

Impact Factor: 4.76 · DOI: 10.1021/ic951587z

Cobalt(II) Substituted Derivatives of *Carcinus maenas* Hemocyanin: Magnetic Characterization, Magnetooptic, and Kinetic Studies Regarding the Geometry of the Active Site

Martina Hüber,[†] Luigi Bubacco,[‡,⊥] Mariano Beltramini,[‡] Benedetto Salvato,[‡] Horst Elias,[§] Jack Peisach,[⊥] Erik Larsen,[∥] Sven E. Harnung,[#] and Wolfgang Haase*,[†]

Institut für Physikalische Chemie, Technische Hochschule Darmstadt, Petersenstrasse 20, 64287 Darmstadt, Germany, Dipartimento Biologia, Università di Padova, Via Trieste 75, 35131 Padova, Italy, Institut für Anorganische Chemie, Technische Hochschule Darmstadt, Petersenstrasse 18, 64287 Darmstadt, Germany, Department of Physiology and Biophysics, Albert Einstein College of Medicine, Yeshiva University, 1300 Morris Park Avenue, Bronx, New York 10467, Chemistry Department, The Royal Veterinary and Agricultural University, Thorvaldsensvej 40, 1871 Frederiksberg C, Copenhagen, Denmark, and Department of Chemistry, University of Copenhagen, Universitetsparken 5, 2100 Copenhagen, Denmark

Received December 13, 1995[⊗]

Mononuclear (Co^{II}−Hc) and dinuclear (Co^{II}_2−Hc) Co(II) substituted derivatives of *Carcinus maenas* hemocyanin (Hc) are characterized by magnetic susceptibility measurements, magnetic circular dichroism spectroscopy, and kinetic experiments with cyanide. Magnetization measurements up to 8 T reveal that the mononuclear Co^{II}−Hc posseses a $S = {}^3/_2$ ground state, demonstrating that the optical properties are consistent with a distorted tetrahedral coordination geometry. The Co^{II}_2−Hc, Co^{II}_2−N_3−Hc, and Co^{II}−Hc derivatives exhibit visible and near-infrared magnetic circular dichroism (MCD) signals and magnetic characteristics which also reflect tetrahedral coordination geometry. Magnetic susceptibility measurements of dinuclear Co^{II}_2−Hc and Co^{II}_2−N_3−Hc reveal strong antiferromagnetic coupling with $|J| > 100$ cm^{-1}, consistent with the existence of a ligand bridging the metal centers. The results of the magnetic susceptibility measurements together with the MCD data imply that the putative bridging ligand of the dinuclear Co^{II}_2−Hc can be substituted by small anions like azide. Otherwise a coordination number higher than 4 would have been achieved. No evidence for an octahedrally coordinated Co(III) species was obtained from magnetic or magnetooptical studies, ruling out the oxidation of Co^{II}_2−Hc to form a Co^{III}−O_2^-−Co^{III} complex and hence dioxygen-binding to Co^{II}_2−Hc. Kinetic investigation of the reaction of dinuclear Co^{II}_2−Hc with excess cyanide by stopped-flow spectrophotometry reveals that the protein adds cyanide in a fast initial equilibrium reaction to form an adduct. This is followed by slow cyanide-assisted removal of the metal ions from the active site in two steps.

Introduction

Hemocyanins are found in many arthropods and molluscs, where they occur extracellularly in the hemolymph. The biological function of these giant proteins is the reversible and cooperative binding of dioxygen at a dinuclear Cu(I) site[1,2] to form a Cu^{II}−O_2^{2-}−Cu^{II} complex, where the two cooper(II) ions show strong antiferromagnetic exchange coupling.[1,3−6] As already predicted by studies on copper−dioxygen model complexes, where physical properties largely resemble those of the native protein,[7−9] the first X-ray crystal structure of oxygenated *Limulus polyphemus* (*L. polyphemus*) subunit II hemocyanin[10] showed that dioxygen is bound symmetrically and equidistantly in a μ-η^2:η^2 bridging structure between two copper atoms. This peroxo bridging structure, which was hitherto unknown for 3d transition metals, explains the strong antiferromagnetic—and hence EPR silent—exchange interaction of $|J| \geq 550$ cm^{-1} (*L. polyphemus*)[6] and $|J| \geq 625$ cm^{-1} (*Megathura crenulata*),[5] respectively. The Cu−Cu distance of 3.6 Å is consistent with previously reported EXAFS data.[11,12] Each metal ion is directly ligated by three histidylimidazole nitrogens. Four equatorial N(His) (His = histidyl) ligands are found in the same plane as the Cu_2O_2 core, and two axially coordinated N(His) complete the coordination sphere of the metal ions.[13−15] The X-ray crystal structure together with recent resonance Raman studies[16] rule out the presence of a postulated ligand additionally bridging the metal ions, as assumed earlier.[17,18]

* Author to whom correspondence should be addressed.
† Institut für Physikalische Chemie, Technische Hochschule Darmstadt.
‡ Università di Padova.
§ Institut für Anorganische Chemie, Technische Hochschule Darmstadt.
⊥ Yeshiva University.
∥ The Royal Veterinary and Agricultural University.
University of Copenhagen.
⊗ Abstract published in *Advance ACS Abstracts,* November 1, 1996.

(1) Freedman, T. B.; Loehr, J. S.; Loehr, T. M. *J. Am. Chem. Soc.* **1976**, *98*, 2809−2815.
(2) Ellerton, D. H.; Ellerton, N. F.; Robinson, H. A. *Prog. Biophys. Mol. Biol.* **1983**, *41*, 143−248.
(3) Van Holde, K. E. *Biochemistry* **1967**, *6*, 93−99.
(4) Moss, T. H.; Gould, D. C.; Ehrenberg, A.; Loehr, J. S.; Mason, H. S. *Biochemistry* **1973**, *12*, 2444−2448.
(5) Solomon, E. I.; Dooley, D. M.; Wang, R.-H.; Gray, H. B.; Cerdonio, M.; Mogno, F.; Romani, G. L. *J. Am. Chem. Soc.* **1976**, *98*, 1029−1031.
(6) Dooley, D. M.; Scott, R. A.; Ellinghaus, J.; Solomon, E. I.; Gray, H. B. *Proc. Natl. Acad. Sci. USA* **1978**, *75*, 3019−3022.
(7) Kitajima, N.; Fujisawa, K.; Moro-oka, Y.; Toriumi, K. *J. Am. Chem. Soc.* **1989**, *111*, 8975−8976.
(8) Kitajima, N.; Fujisawa, K.; Fujimoto, C.; Moro-oka, Y.; Hashimoto, S.; Kitagawa, T.; Toriumi, K.; Tatsumi, K.; Nakamura, A. *J. Am. Chem. Soc.* **1992**, *114*, 1277−1291.
(9) Kitajima, N.; Moro-oka, Y. *Chem. Rev.* **1994**, *94*, 737−757.
(10) Magnus, K. A.; Hazes, B.; Ton-That, H.; Bonaventura, C.; Bonaventura, J.; Hol, W. G. J. *Proteins* **1994**, *19*, 302−309.
(11) Brown, J. M.; Powers, L.; Kincaid, B.; Larrabee, J. A.; Spiro, T. G. *J. Am. Chem. Soc.* **1980**, *103*, 984−986.
(12) Woolery, G. L.; Powers, L.; Winkler, M.; Solomon, E. I.; Spiro, T. G. *J. Am. Chem. Soc.* **1984**, *106*, 86−92.

S0020-1669(95)01587-4 CCC: $12.00

Upon deoxygenation the coordination number for each copper decreases from 5 to 3. For the *L. polyphemus* protein the coordination geometry changes from square pyramidal in oxyhemocyanin to trigonal planar in deoxyhemocyanin[19].

To further obtain information about geometry, chemical reactivity, and flexibility of the active site structure in hemocyanin, the spectroscopically silent Cu(I) has been replaced by Co(II).[21−24] The rationale for this replacement is based on the high sensitivity of the physical properties of Co(II) on ligand composition and coordination geometry, which can be monitored by magnetic and optical spectroscopic methods. This paper describes studies of a series of Co(II) substituted hemocyanin derivatives of the arthropod *Carcinus maenas* (*C. maenas*) hemocyanin (Hc) containing both a mononuclear and a dinuclear metal center. X-ray absorption near edge structure spectroscopy (XANES)[25] and low-temperature optical spectroscopic studies[26] of the mononuclear and dinuclear derivatives revealed a four-coordinate metal binding site for each metal ion, showing tetrahedral (Co^{II}_2−Hc) and distorted tetrahedral (Co^{II}−Hc, Cu^{I}−Co^{II}−Hc) geometry, respectively. Earlier studies on Co(II)-substituted *L. polyphemus* hemocyanin[21,23,24,27] had also suggested a tetrahedral binding site for the metal ions, although the influence of adventitiously bound Co(II) had not been adequately considered in active site characterization.[28]

This present investigation contributes to the detailed characterization of the active site of Co(II) substituted derivatives of *C. maenas* Hc. Because the coordination chemistry of copper and cobalt is different in detail, one motivation for the present study is to compare some properties of Hc and Co(II) substituted Hc in specific features, allowing for some structural proposals of Co(II) substituted Hcs, but also to gain a feeling about the flexibility and chemical reactivity abilities of the active site in general. Besides deeper understanding regarding structural differences in the coordination geometry of the mononuclear derivative compared to the dinuclear derivative, the question of dioxygen uptake is considered.

Regarding the structure of the dinuclear Co(II) substituted derivative, the presence of a ligand bridging the metal ions mediating a coupled metal site is suggested. The presence of a bridging ligand was also postulated from magnetic susceptibility measurements on Co(II) substituted *L. polyphemus* hemocyanin. In this present study, the magnetic properties of dinuclear Co(II) substituted derivatives of *C. maenas* hemocyanin are investigated and the question of whether ligand substitution leads to the loss of the bridging ligand is considered.

In order to obtain information about the reactivity of Co(II) substituted hemocyanin with exogenous ligands, the kinetics of the reaction of Co^{II}_2−Hc with cyanide was studied. This reaction is of special interest, since ligands like azide, chloride, and thiocyanate are capable of binding the Co(II) substituted active site, but only cyanide can both coordinate and remove the metal.[22,28]

Materials and Methods

Sample Preparation. All samples were prepared from purified *C. maenas* apohemocyanin.[28] Metal incorporation into the apoprotein leads either to a stable mononuclear derivative, Co^{II}−Hc, or to a dinuclear derivative, Co^{II}_2−Hc.[28] Extensive dialysis against 5 mM sodium phosphate buffer (pH 7), containing 2 mM ethylenediaminetetraacetic acid (EDTA), yields protein samples, without adventitiously bound Co(II). Synthesis and detailed characterization of the Hc derivates was previously described.[28] Co^{II}_2−N_3−Hc was prepared from the dinuclear derivative Co^{II}_2−Hc by extensive dialysis against a 100 mM solution of sodium azide in 50 mM Tris/HCl buffer, pH 7. Sucrose, 18% (w/w), was added to concentrated protein solutions in 50 mM Tris/HCl buffer (pH 7) prior to storage at −20 °C. Lyophylized samples were prepared from protein solutions in 5 mM sodium phosphate buffer (pH 7), containing 1:2 (w/w) sucrose. The Co and Cu concentrations were determined by atomic absorption spectroscopy, equipped for graphite furnance analysis.[28] The copper content in the Co(II) substituted derivatives was less than 2% of that found in holohemocyanin. Protein concentrations were determined spectrophotometrically at 278 nm, using the absorptivity $\epsilon_{278} = 93\,000\ M^{-1}\ cm^{-1}$, which refers to the monomeric subunit molecular weight of 75 000 per active site.[28]

Magnetic Measurements. Due to the high molecular weight of 75 000 per active site the diamagnetic contribution of the protein matrix is large compared to contributions of the paramagnetic metal ions. Therefore determination of the diamagnetic correction plays an important role in assessing the absolute value of the magnetic susceptibility of the protein. Furthermore the contribution of small paramagnetic impurities embodied in the quartz sample holder and residual Cu(II) in the sample have to be considered. The approach used was to measure the apoprotein as well as the quartz sample holder independently. The data were then used for the diamagnetic corrections for the Co(II) substituted protein samples.

Variable temperature magnetic susceptibility measurements in the range 4.2−300 K were performed using a Faraday type magnetic balance. The magnetometer was equipped with a Cahn D-200 microbalance, having a resolution of 0.1 μg, and a Bruker B-MN 200/60 electromagnet, described elsewhere.[29] The applied magnetic field was 1.56 T. The samples consisted of lyophilized protein as well as of concentrated protein samples, contained in a quartz sample holder. $HgCo(SCN)_4$ was used as a calibrant.

Magnetization Measurements. Field dependent magnetization data were collected at 4.2 K using a Faraday system consisting of an superconducting magnet (Oxford Instruments) with a main field up to 8 T and a maximum gradient field of 10 T m^{-1} at 4.2 K. The system was equipped with a Cahn D-200 microbalance having a resolution of 0.1 μg. $HgCo(SCN)_4$ was used as calibrant as before. The concentrated protein solutions used in the study were kept in a closed aluminium container to prevent sublimation of the frozen sample during the measurement. Magnetization data of the sample container and the apoprotein were determined under the same conditions as those for the cobalt containing sample.

(13) Volbeda, A.; Hol, W. G. J. *J. Mol. Biol.* **1989**, *206*, 531−546.
(14) Volbeda, A.; Hol, W. G. J. *J. Mol. Biol.* **1989**, *209*, 249−279.
(15) Hazes, B.; Magnus, K. A.; Bonaventura, C.; Bonaventura, J.; Dauter, Z.; Kalk, K. H.; Hol, W. G. J. *Protein Sci.* **1993**, *2*, 597−619.
(16) Ling, J.; Nestor, L. P.; Czernuszewicz, R. S.; Spiro, T. G.; Fraczkiewicz, R.; Sharma, K. D.; Loehr, T. M.; Sanders-Loehr, J. *J. Am. Chem. Soc.* **1994**, *116*, 7682−7691.
(17) Eickman, N. C.; Himmelwright, R. S.; Solomon, E. I. *Proc. Natl. Acad. Sci. USA* **1979**, *76*, 2094−2098.
(18) Himmelwright, R. S.; Eickman, N. C.; LuBien, C. D.; Solomon, E. I. *J. Am. Chem. Soc.* **1980**, *102*, 5378−5388.
(19) Magnus, K. A.; Ton-That, H.; Carpenter, J. E. *Chem. Rev.* **1994**, *94*, 727−735.
(20) Suzuki, S.; Kino, J.; Kimura, M.; Mori, W.; Nakahara, A. *Inorg. Chim. Acta* **1982**, *66*, 41−47.
(21) Suzuki, S.; Kino, J.; Nakahara, A. *Bull. Chem. Soc. Jpn.* **1982**, *55*, 212−217.
(22) Salvato, B.; Beltramini, M.; Piazzesi, A.; Alviggi, M.; Ricchelli, F.; Magliozzo, R. S.; Peisach, J. *Inorg. Chim. Acta* **1986**, *125*, 55−66.
(23) Lorösch, J.; Haase, W. *Biochemistry* **1986**, *25*, 5850−5857.
(24) Dutton, T. J.; Baumann, T. F.; Larrabee, J. *A. Inorg. Chem.* **1990**, *29*, 2272−2278.
(25) Della Longa, S.; Bianconi, A.; Palladino, L.; Simonelli, B.; Congiu Castellano, A.; Borghi, E.; Barteri, M.; Beltramini, M.; Rocco, G. P.; Salvato, B.; Bubacco, L.; Magliozzo, R. S.; Peisach, J. *Biophys. J.* **1993**, *65*, 2680−2691.
(26) Vitrano, E.; Cupane, A.; Leone, M.; Militello, V.; Cordone, L.; Salvato, B.; Beltramini, M.; Bubacco, L.; Rocco, G. P. *Eur. Biophys. J.* **1993**, *22*, 157−167.
(27) Larrabee, J. A.; Baumann, T. F.; Chisdes, S. J.; Lyons, T. J. *Inorg. Chem.* **1992**, *31*, 3630−3635.
(28) Bubacco, L.; Magliozzo, R. S.; Beltramini, M.; Salvato, B.; Peisach, J. *Biochemistry* **1992**, *31*, 9294−9303.
(29) Gehring, S.; Fleischhauer, P.; Paulus, H.; Haase, W. *Inorg. Chem.* **1993**, *32*, 54−60.

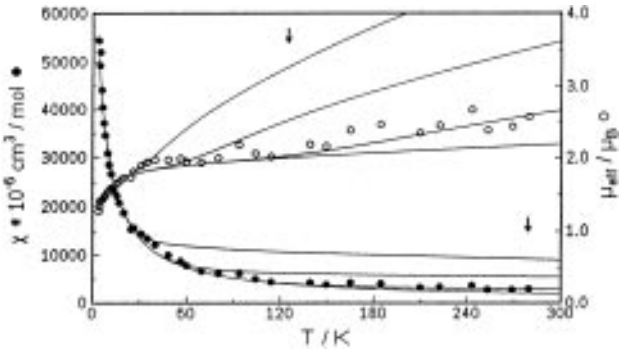

Figure 1. Temperature dependence of magnetic susceptibility (●) and magnetic moment (○) for a lyophilized sample of Co^{II}_2−Hc. The data are expressed per Co(II). The solid lines simulate calculations for $-J = 50$, 100, 241, and 1000 cm^{-1}. The arrows indicate increasing values of $|J|$.

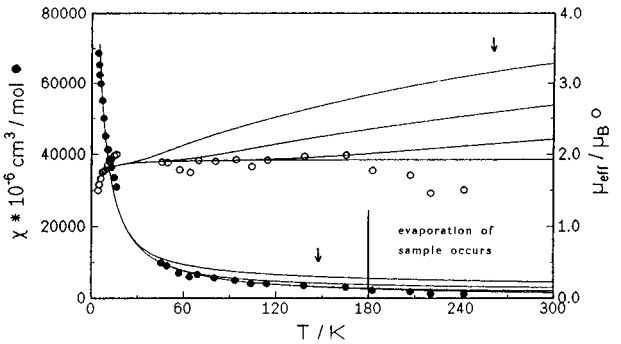

Figure 2. Temperature dependence of magnetic susceptibility (●) and magnetic moment (○) for a concentrated solution of Co^{II}_2−N_3−Hc. The data are expressed per Co(II). The solid lines simulate calculations for $-J = 50$, 100, 219, and 1000 cm^{-1}. The arrows indicate increasing values of $|J|$.

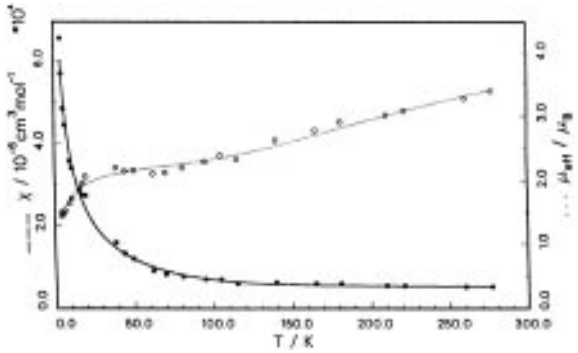

Figure 3. Temperature dependence of magnetic susceptibility (●) and magnetic moment (○) for a lyophilized sample of Co^{II}−Hc. The best fit is illustrated as a solid line with $g = 2.23$, J(paramagnetic species) $= -191$ cm^{-1}, $\Theta = -10.39$ K, TIP $= 474 \times 10^{-6}$ cm^3 mol^{-1}, P(main compound) $= 12.5\%$, and P(paramagnetic species) $= 1.9\%$. (J(paramagnetic species) refers to the impurity of Co^{II}_2−Hc.

Magnetic Circular Dichroism Spectroscopy. Room temperature visible magnetic circular dichroism (MCD) spectra were obtained on a JASCO J-710 spectropolarimeter, equipped with a 1.6 T permanent magnet.

Measurements in the near-infrared region were performed at 1.1 T on a specially designed instrument.

Spectra were recorded on 1.56 mM Co^{II}_2−Hc, 1.66 mM Co^{II}_2−N_3−Hc, and 1.54 mM Co^{II}−Hc solutions, prepared in 0.1 M Tris/HCl buffer, pH 8.

MCD spectra at 4 T and at 4.2 K were measured using a modified Cary 14 spectropolarimeter equipped with an Oxford Instruments superconducting magnet.[30] The spectra were obtained on a thin protein film, obtained from a mixture of a concentrated protein sample and polyvinyl alcohol.

All MCD spectra were corrected for the presence of natural optical activity.

Kinetic Measurements. Kinetic experiments were performed with a conventional stopped-flow spectrophotometer (Durrum, D-110), equipped with a modified thermostating system.[31] Buffered solutions of 8.79×10^{-3} mM Co^{II}_2−Hc (0.1 M Tris/HCl, pH 8) were reacted with buffered solutions of cyanide (0.1 M Tris/HCl, pH 8). The concentrations of the cyanide solutions were at least 10-fold higher than that of the protein and with an ionic strength of 0.1 M. The reaction was monitored at 25 °C by following the change in Co(II) absorbance at 560 nm as a function of time.

Results

Magnetic Measurements. The magnetic susceptibility χ and the magnetic moments μ_B, per mole of Co(II), of lyophilized samples of Co^{II}_2−Hc and Co^{II}−Hc as well as of a concentrated solution of Co^{II}_2−N_3−Hc, as a function of temperature, are displayed in Figures 1−3. The (best) fit calculated (see below) is illustrated as a solid line.

In order to rule out the possibility that the active site is altered by lyophilization, lyophilized samples of Co^{II}_2−Hc and Co^{II}−Hc as well as concentrated solutions of both derivatives were investigated. For both lyophilized and solution samples consistent experimental magnetic susceptibility data were obtained.

The susceptibility data for Co^{II}_2−Hc and Co^{II}_2−N_3−Hc were computer fitted by a least squares method to a theoretical expression based on the Hamiltonian $\hat{H} = -2J\hat{S}_1\cdot\hat{S}_2$ for isotropic exchange of $S_1 = S_2 = {}^3/_2$. This equation was modified to include contributions of small amounts of paramagnetic impurities P exhibiting Curie behavior, arising from uncoupled metal ions or from vacancies in the dinuclear active sites. In the concentrated solutions the presence of dissolved dioxygen may additionally contribute to the overall paramagnetic susceptibility. Furthermore, a term accounting for the temperature independent paramagnetism (TIP) was included, leading to

$$\chi_{calc} = (1 - P)\left[\frac{C}{T - \Theta} f(J,T)\right] + P\frac{C}{T} + \text{TIP} \qquad (1)$$

with $C = N_A g^2 \mu_B^2/3k$ (C, Curie constant; Θ, Weiss constant; N_A, Avogadro number; g, Landé factor; μ_B, Bohr magneton; k, Boltzmann constant) and $f(J,T)$ is given in the literature.[32]

The results of the best fits obtained by a computer aided procedure are summarized in Table 1.

The magnetic properties of lyophilized mononuclear Co^{II}−Hc are displayed in Figure 3, showing molar magnetic susceptibility vs temperature. In order to obtain a good fit to the Curie−Weiss law behavior of a $S = {}^3/_2$ metal center, an additional term had to be included that accounted for the presence of a coupled dinuclear $S_1 = S_2 = {}^3/_2$ metal center (paramagnetic species) as described above. Further improvement in the quality of the fit was obtained by the introduction of a term referring to paramagnetic impurities and a term for the TIP.

$$\chi(T) = (1 - P(\text{main compound}))\frac{C}{T}(i) + P(\text{main compound})\frac{2C}{T - \Theta}(1.25) + \text{TIP} \quad (2)$$

with

(30) Crans, D. C.; Harnung, S. E.; Larsen, E.; Shin, P.-K.; Theisen, L. A.; Trabjerg, I. *Acta Chem. Scand.* **1991**, *45*, 456−462.

(31) Fröhn, U.; von Irmer, A.; Wannowius, K. J.; Elias, H. *Inorg. Chem.* **1980**, *19*, 869−875.

(32) O'Connor, J. C. *Prog. Inorg. Chem.* **1982**, *29*, 203−283.

Table 1. Summary of Temperature Dependent Magnetic Susceptibility Results of Lyophilized Samples and Solutions of Co(II) Substituted Hemocyanin Derivatives

protein sample	sample form	J/cm^{-1}	g	Θ/K	TIP/(10^{-6} cm^{-3} mol^{-1})	P/%
Co^{II}_2−Hc	lyophilized solution	−241	2.30	−5.0	499	9.16
		−230	2.23	−2.88	282	29.3
Co^{II}_2−N_3−Hc	solution	−219	2.25	−1.56		19.7
Co^{II}−Hc	lyophilized					
	A		2.23	−10.39	474	12.5[a]
	B	−191				1.9
	solution					
	A		2.20	−6.91	111	7.3[a]
	B	−229				7.4

[a] Amount of paramagnetic species: A, main compound; B, paramagnetic species.

$$i = 2P(\text{paramagnetic species})f(J,T) \qquad (3)$$

and $C = N_A g^2 \mu_B^2/3k$. $f(J,T)$ is given in the literature.[32]

Magnetization Measurements of Mononuclear Cobalt(II) Hemocyanin. The field dependent magnetization up to 8 T at 4.2 K is presented in Figure 4, where the magnetization M is plotted vs the magnetic field B (T). The data were corrected for the contribution of the sample container, which was determined over the same interval of applied magnetic fields. The experimental data approach saturation, following the behavior of a typical Brillouin function of a $S = {}^3/_2$ ground state. The theoretical expression (eqs 4−6)[33]

$$M = N_A g \mu_B S B_s(\eta) \qquad (4)$$

N_A, Avogadro number; g, Landé factor; μ_B, Bohr magneton; S, quantum number; $B_s(\eta)$, Brillouin function

where the Brillouin function is defined as

$$B_s(\eta) = \frac{1}{S}\left[\left(S + \frac{1}{2}\right)\coth\left(\left(S + \frac{1}{2}\right)\eta\right) - \frac{1}{2}\coth\left(\frac{\eta}{2}\right)\right] \qquad (5)$$

with

$$\eta = g\mu_B B/kT$$

B, Magnetic field strength; k, Boltzmann constant

was applied for calculating the field dependence of the magnetization for a $S = {}^3/_2$ spin state with $g = 2.0$ (shown as a solid line). The experimental data are well-described by this theoretical expression, showing that the active site of the mononuclear derivative consists of a high-spin, $S = {}^3/_2$ Co(II) center.

Magnetic Circular Dichroism Spectroscopy. The MCD spectra in the 1.4−2.2 μm^{-1} region of Co^{II}_2−Hc, Co^{II}_2−N_3−Hc, and Co^{II}−Hc at room temperature as well as the Co^{II}_2−Hc MCD spectrum at 4.2 K are shown in Figure 5A−C (upper panels) and Figure 6, respectively; the corresponding energies of the band maxima are presented in Table 2. In addition, the optical absorption spectra are displayed (Figures 5, lower panels) to allow a comparison with the absorption maxima previously discussed in the literature.[26,28] In Figure 7A−C) the near-infrared MCD spectra are displayed.

The major features of the visible MCD spectra consist of one large positive and one large negative band that correspond to the absorption maxima. The spectra observed for Co^{II}_2−Hc and Co^{II}_2−N_3−Hc show strong similarities; the band pattern, magnitude, and sign of the MCD signal are closely comparable. The maxima of the two prominent bands are located at 1.825 and 1.656 μm^{-1} for Co^{II}_2−Hc, and at 1.832 and 1.656 μm^{-1} for Co^{II}_2−N_3−Hc. The low-temperature spectrum of Co^{II}_2−Hc shows that the observed overall band shape seen at room temperature is retained. The bands gain intensity with lowered temperature and are slightly blue-shifted to 1.852 and 1.701 μm^{-1}.

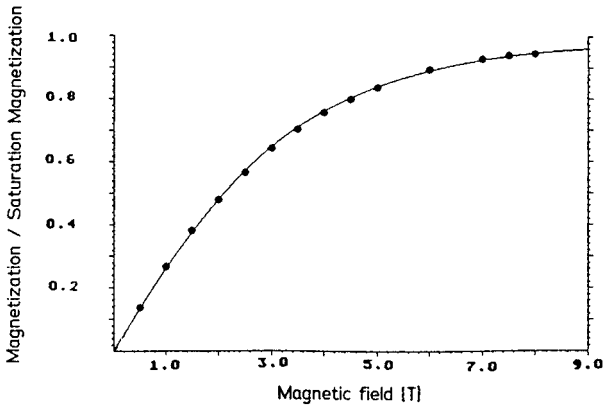

Figure 4. Plot of the magnetization M of Co^{II}−Hc vs the magnetic field B of Co^{II}−Hc. The experimental data (●) follow a Brillouin function for $S = {}^3/_2$ (−).

In contrast to the MCD signals of the Co^{II}_2 derivatives, the MCD spectrum of the mononuclear Co^{II}−Hc is broadened (Figure 5A−C). The band maxima of the mononuclear derivative are centered at 1.905 and 1.698 μm^{-1}. Again, the band shapes are comparable, while the band maxima of the mononuclear derivative are clearly shifted toward higher energies with respect to those of the dinuclear derivatives.

The near-infrared MCD spectra of Co^{II}_2−Hc, Co^{II}_2−N_3−Hc, and Co^{II}−Hc show two broad bands with opposite signs, located at 0.943 and 0.745 μm^{-1} (Co^{II}_2−Hc), at 0.963 and 0.745 μm^{-1} (Co^{II}_2−N_3−Hc), and at 0.953 and 0.755 μm^{-1} (Co^{II}−Hc) (see Table 3).

Since the energies of the ν_2 and ν_3 transitions can be estimated from the MCD spectra,[34] it is possible to calculate the strength of the ligand field Δ_t from eq 6, neglecting spin−orbit interactions.[35]

$$\Delta_t^2 - 0.529(\nu_2 + \nu_3)\Delta_t + 0.294\nu_2\nu_3 = 0 \qquad (6)$$

The term energies ν_2 and ν_3 are obtained by averaging the positions of the positive and negative MCD bands.[34] Assuming $\nu_2 \pm 0.05$ μm^{-1} and $\nu_3 \pm 0.03$ μm^{-1}, according to (6) a value of $\Delta_t = 5000 \pm 300$ cm^{-1} was calculated for the Co(II) substituted derivatives.

(33) Carlin, R. L. *Magnetochemistry*; Springer Verlag: Berlin, 1986.

(34) Solomon, E. I.; Rawlings, J.; Mc Millin, D. R.; Stephens, P. J.; Gray, H. B. *J. Am. Chem. Soc.* **1976**, *98*, 8047−8048.

(35) Lane, R. W.; Ibers, J. A.; Frankel, R. B.; Papaefthymiou, G. C.; Holm, R. H. *J. Am. Chem. Soc.* **1977**, *99*, 84−98.

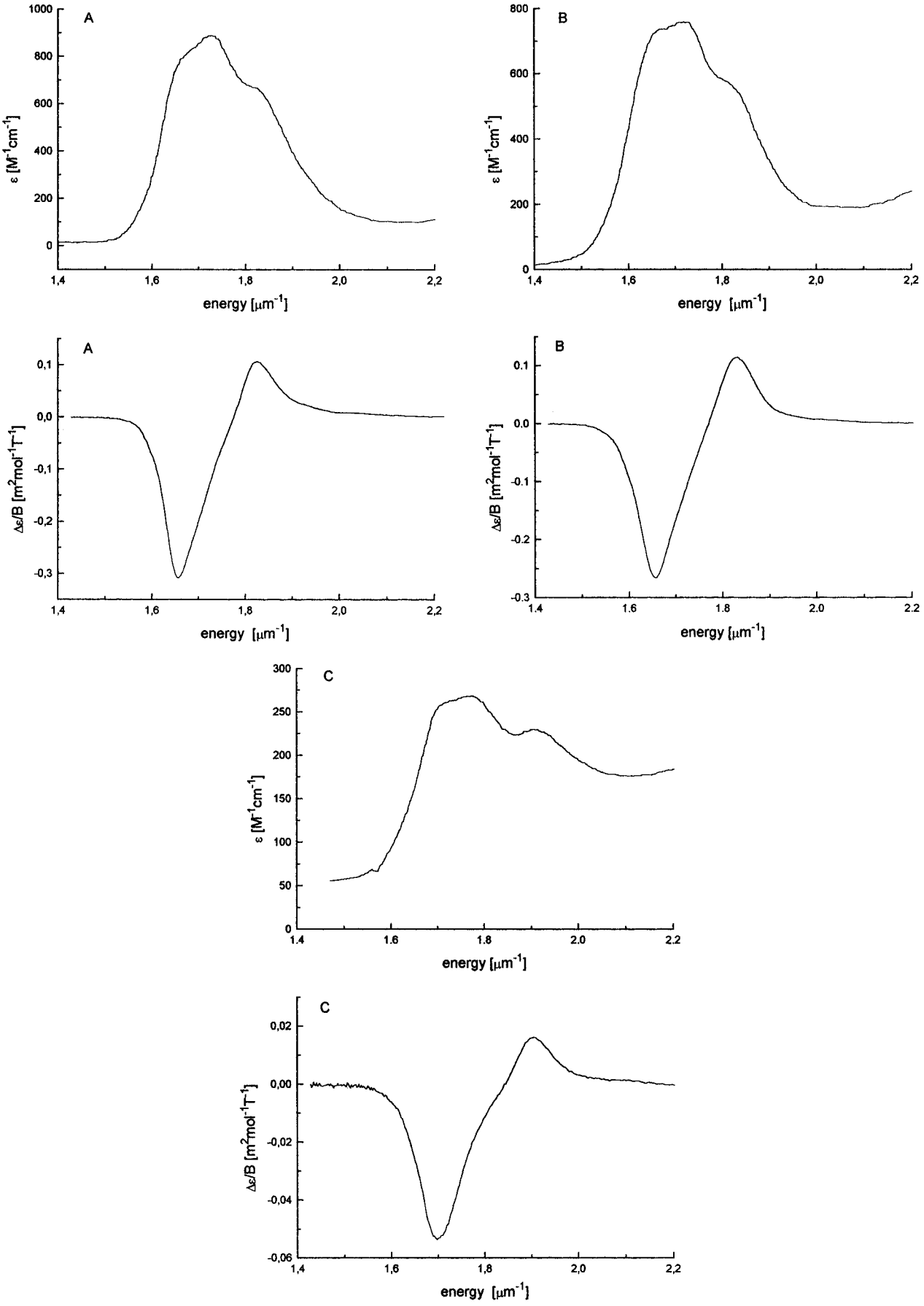

Figure 5. (A−C) Optical absorption (upper) and MCD spectra (lower) of (A) Co^{II}_2−Hc, (B) Co^{II}_2−N_3−Hc, and (C) Co^{II}−Hc at room temperature (0.1 M Tris/HCl buffer, pH 8).

Kinetic Measurements. As shown in Figure 8, the reaction of Co^{II}_2−Hc with a 100-fold excess of cyanide is a three step process. An initial fast increase in absorbance at 560 nm is followed by two much slower steps, associated with a decrease

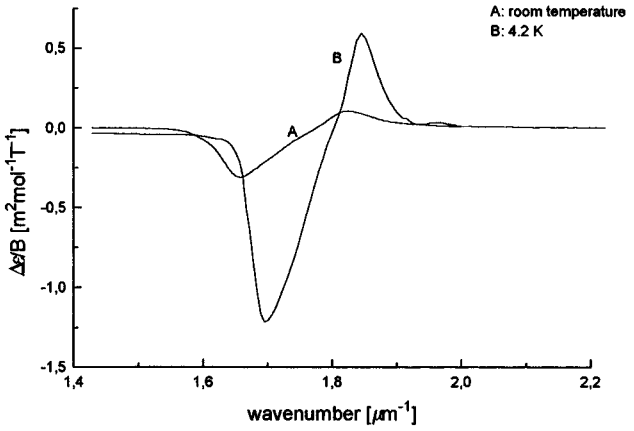

Figure 6. MCD spectra of Co^{II}_2−Hc at room temperature (A) and at 4.2 K (B).

in absorbance. The absorbance/time data of the overall reaction can be fitted to eq 7. The amplitudes A and rate constants k_{obsd}

$$A = \Delta A_1[-k_{obsd.1}t] + \Delta A_2[-k_{obsd.2}t] + \Delta A_3[-k_{obsd.3}t] + A_\infty \quad (7)$$

obtained at variable concentrations of cyanide are summarized in Table 4. It follows for the experimental rate constants that, at a given cyanide concentration, $k_{obsd.1} \gg k_{obsd.2} > k_{obsd.3}$. The cyanide dependence of both the amplitudes and rate constants suggests that sequence 8 is an adequate description of the overall

$$Co^{II}_2\text{−Hc} \underset{K_1}{\overset{+CN^-}{\rightleftharpoons}} \text{adduct} \underset{K_2}{\overset{+CN^-}{\rightleftharpoons}} \text{intermediate} \xrightarrow[k_3]{+CN^-} \text{product} \quad (8)$$

process. Excess cyanide removes copper from hemocyanin. It is therefore reasonable to assume that the decrease in absorbance, as observed for the second and third steps of sequence 8, describes the cyanide-induced removal of cobalt from the protein. If so, it makes sense to further assume that the initial fast increase in absorbance is due to cyanide addition to the active site of Co^{II}_2−Hc according to (9).

$$Co^{II}_2\text{−Hc} + CN^- \overset{K_1}{\rightleftharpoons} \text{adduct} \quad (9)$$

Figure 9 shows the visible spectrum of the adduct and of the final product in comparison with that of Co^{II}_2−Hc.

For $[CN^-] \geq 0.005$ M, the amplitude ΔA_1 for the first step in (8) is constant within the limits of error. This means that equilibrium 9 is completely shifted to the adduct side and adduct formation can hence be described as an irreversible pseudo-first-order process according to (10) and (11),with A_{ad} being

$$\text{d[adduct]}/\text{d}t = k_{obsd.1}[Co^{II}_2\text{−Hc}] \quad (10)$$

$$A = \Delta A_1 \exp[-k_{obsd.1}t] + A_{ad} \quad (11)$$

the absorbance of the adduct at $[\text{adduct}] = [Co^{II}_2\text{−Hc}]_0$ and $\Delta A_1 = A_{ad} - A_0$ (A_0 = absorbance of Co^{II}_2−Hc at $[Co^{II}\text{−Hc}]_0$).

It follows from the plot of $k_{obsd.1}$ vs $[CN^-]$ (see Figure 10) that the increase in $k_{obsd.1}$ is of the saturation type. This suggests that cyanide addition is preceded by outer-sphere complexation according to (12) and (13). If so, the dependence $k_{obsd.1} =$

$$Co^{II}_2\text{−Hc} + CN^- \overset{K_{os}}{\rightleftharpoons} \{Co^{II}_2\text{−Hc}, CN^-\} \quad (12)$$

$$\{Co^{II}_2\text{−Hc}, CN^-\} \xrightarrow{k_{ad}} \text{adduct} \quad (13)$$

$f([CN^-])$ should follow relationship (14). Fitting of (14) to the

$$k_{obsd.1} = \frac{k_{ad}K_{os}[CN^-]}{1 + K_{os}[CN^-]} \quad (14)$$

$k_{obsd.1}/[CN^-]$ data obtained leads to the solid line shown in Figure 10 with $k_{ad} = 256 \pm 10$ s^{-1} and $K_{os} = 62 \pm 8$ M^{-1}.

The sum of the data obtained form the amplitude ΔA_1 at variable cyanide concentration (see Table 4) allows an estimate of the equilibrium constant K_1 for adduct formation according to (9). At $[CN^-] < 0.005$ M, the size of ΔA_1 is cyanide-dependent. It is to be expected that ΔA_1 follows relationship (15). Figure 11 shows the plot of ΔA_1 vs $\log[CN^-]$ with the

$$\Delta A_1 = \frac{(A_{ad} - A_0)K_1[CN^-]}{1 + K_1[CN^-]} \quad (15)$$

solid (and broken) line representing the result of fitting (15) to the data. The fitting parameters are $K_1 = 2100 \pm 400$ M^{-1} and $(A_{ad} - A_0) = (8.0 \pm 0.2) \times 10^{-2}$.

Discussion

Magnetic Susceptibility Measurements. Variable temperature magnetic susceptibility measurements using lyophilized protein samples bear many advantages as compared to carrying out measurements on protein solutions. The sample weight under vacuum can be correctly determined at room temperature. By removal of the water from a protein sample, a higher concentration per volume sample holder is achieved, which consequently leads to greater sensitivity. Furthermore the measurements can be carried out over a larger temperature range, while for solutions the temperature range is limited to 180−200 K. At temperatures higher than 200 K frozen solutions start melting, and since the measurements are carried out at low pressure (530 Pa helium atmosphere), this is accompanied by evaporation of the samples.

To be sure that the active site is not altered in lyophilized samples, comparative measurements were carried out using concentrated protein solutions. It should be noted (Table 1) that both types of samples show comparable magnetic behavior, demonstrating that the active site remains intact in the lyophilized protein forms. This is in accordance with earlier observations by Della Longa et al.[25] It should be noted that the difference in the set of data obtained for lyophilized samples and protein solutions (Table 1) is not significant. Due to the high scattering of the experimental data points, small variations of one single parameter lead to a different set of parameters, which also represents a good fit. However, within the experimental error consistent magnetic data are obtained.

Co^{II}_2−Hc, Co^{II}_2−N_3−Hc. The magnetic data are consistent with a dinuclear Co(II), $S_1 = S_2 = {}^3/_2$ metal site exhibiting strong exchange coupling. Variations of the coupling constant are shown in Figures 1 and 2. Taking into account the experimental error, the lower limit of the antiferromagnetic exchange coupling constant is estimated to be $|J| > 100$ cm^{-1} for Co^{II}_2−Hc and $|J| > 100$ cm^{-1} for Co^{II}_2−N_3−Hc ($H = -2J\hat{S}_1\cdot\hat{S}_2$). The magnetic coupling can be explained with the assumption of either a direct magnetic exchange or a superexchange mechanism, involving at least one bridging ligand between the Co(II) ions. X-ray data for oxyhemocyanin have shown a Cu−Cu distance of 3.6 Å.[10] Assuming that replacing the copper with cobalt does not lead to drastic changes of the metal−metal distance, as supported by EXAFS, which show a Co−Co distance of 3.56 ± 0.06 Å.[53] This distance is too large to involve a direct magnetic exchange mechanism. For a superexchange mechanism the molecular orbitals of a putative bridging ligand contribute to the magnetic molecular orbitals of the metal ions,

Table 2. MCD and Optical Spectra Absorption Bands in the Visible Region of Various Co(II) Substituted Hemocyanin Derivatives[a]

protein sample	absorption spectrum/μm^{-1} (nm)	$\epsilon/(M^{-1}\,cm^{-1})$	MCD spectrum/μm^{-1} (nm)	$\Delta\epsilon/B/(m^2\,M^{-1}\,T^{-1})$
Co^{II}_2−Hc	1.815 (551)	672	1.825 (548)	0.106
	1.712 (584)	888	1.656 (604)	−0.310
	1.661 (602)	795		
Co^{II}_2−N_3−Hc	1.822 (549)	578	1.832 (546)	0.114
	1.718 (582)	759	1.656 (604)	−0.266
	1.666 (601)	730		
Co^{II}−Hc	1.916 (522)	229	1.905 (525)	0.016
	1.773 (564)	269	1.698 (589)	−0.053
	1.715 (583)	259		
Co^{II}_2−Hc (film)	1.812 (552)		1.852 (540)[b]	0.594[b]
	1.701 (588)		1.701 (588)[b]	−1.201[b]
	1.661 (602)			

[a] The absorptivity is expressed per active site Co(II). [b] Data collected at 4.2 K.

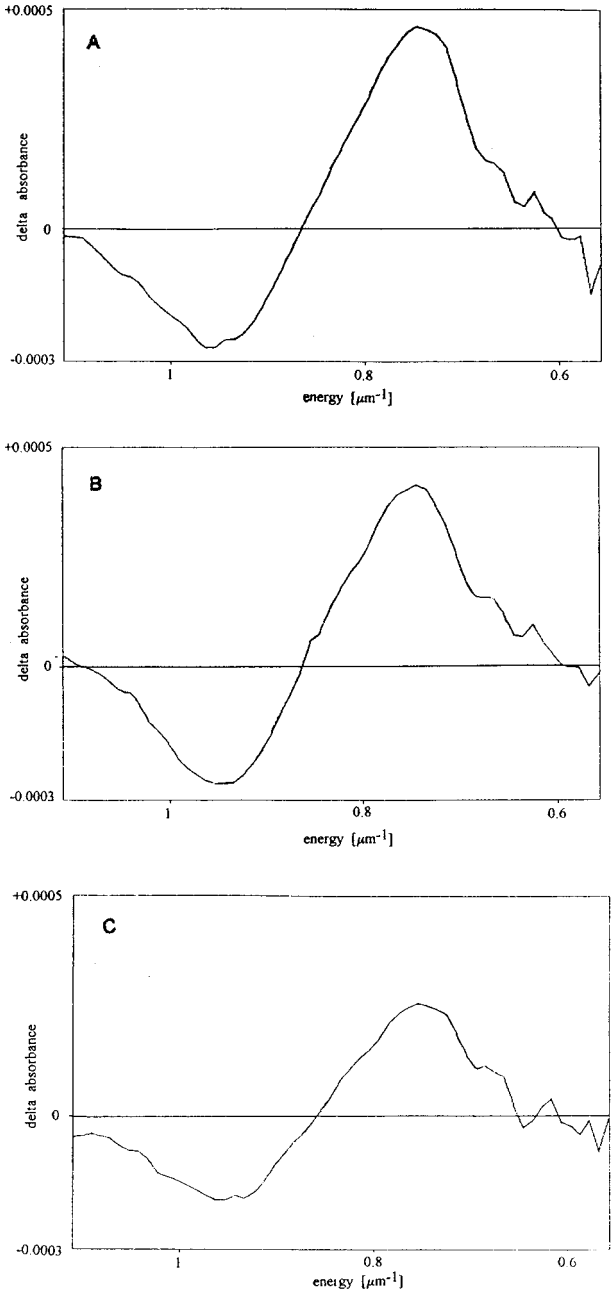

Figure 7. (A−C) Near-infrared MCD spectra of (A) 1.56 mM Co^{II}_2−Hc, (B) 1.66 mM Co^{II}_2−N_3−Hc, and (C) 1.54 mM Co^{II}−Hc at room temperature (0.1 M Tris/HCl buffer, pH 8).

forming a pathway that modulates the magnetic exchange. In this way magnetic exchange is possible over distances that are larger than those for a direct exchange mechanism. Hence, the antiferromagnetic coupling within the dinuclear active site can

Table 3. MCD and Optical Absorption Bands (Spectra Not Shown) in the Near-Infrared Region of Various Co(II) Substituted Hemocyanin Derivatives

protein sample	absorption spectrum/μm^{-1} (nm)	MCD spectrum/μm^{-1} (nm)
Co^{II}_2−Hc	0.951 sh (1051)	0.943 (1060)
	0.891 (1180)	*0.854 (1171)*[a]
		0.745 (1342)
Co^{II}_2−N_3−Hc	0.959 sh (1043)	0.963 (1038)
	0.841 (1189)	*0.864 (1157)*[a]
		0.745 (1342)
Co^{II}−Hc	0.939 sh (1065)	0.953 (1049)
	0.839 (1191)	*0.854 (1171)*[a]
		0.755 (1324)

[a] $\Delta A = 0$.

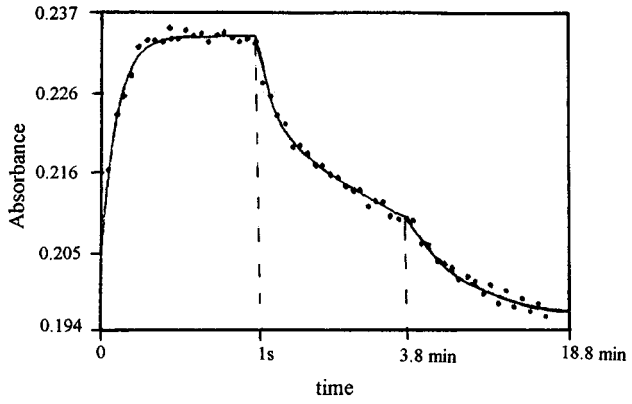

Figure 8. Time dependence of the absorbance at 560 nm for the reaction of Co^{II}_2−Hc (8.8×10^{-5} M) with cyanide (0.01 M) at pH 8 and 25 °C (solid line obtained by computer fitting to eq 7).

best be explained with assumption of a superexchange mechanism involving a bridging ligand with aquo or hydroxy as a plausible choice. For Co^{II}_2−Hc the presence of a bridging ligand is consistent with the antiferromagnetically coupled dinuclear copper site in oxyhemocyanin, where peroxide is the bridging ligand. Here, strong antiferromagnetic coupling was also found. The lower limit of the antiferromagnetic exchange coupling in oxy-Hc was estimated there as $|J| \geq 550\ cm^{-1}$ (*L. polyphemus* Hc)[6] and $|J| \geq 625\ cm^{-1}$ (*Megathura crenulata* Hc).[5] In the low-temperature EPR spectra of Co^{II}_2−Hc a broad low-field absorption at $g \sim 13$ was observed, which was not present for the mononuclear derivative. This signal was attributed to a coupled metal site.[28] Furthermore due to the loss of EPR signal intensity for Co^{II}_2−Hc as compared to Co^{II}−Hc, antiferromagnetic coupling was assumed, possibly achieved by a bridging ligand.[28] This mechanism is supporting the magnetic data which proves strong antiferromagnetic coupling mediated by a bridging ligand. Thus, the assignment of the low-field signal to exchange coupling is strongly supported.

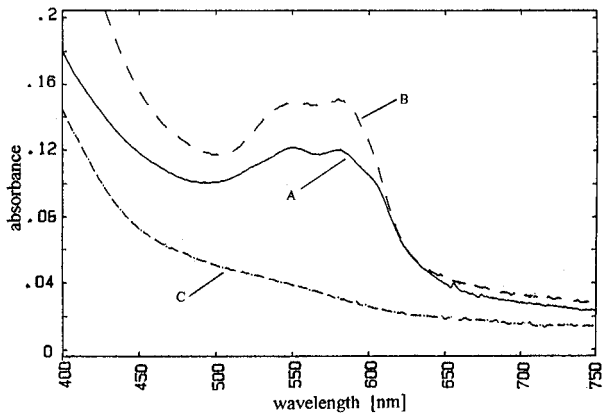

Figure 9. Visible spectra of Co^{II}_2−Hc (A), adduct (B), and product (C) formed according to sequence 8 upon addition of 3.6×10^{-3} M cyanide (B) and 9.4×10^{-2} M cyanide (C) to Co^{II}_2−Hc (1.8×10^{-4} M) at 25 °C and pH 8.

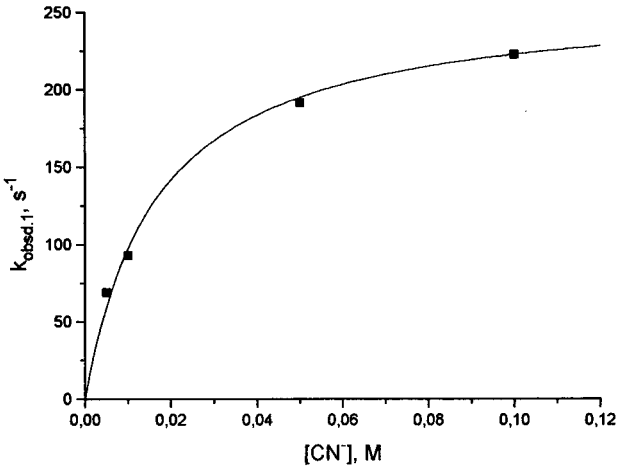

Figure 10. Plot of the dependence of the experimental rate constant $k_{obsd.1}$ on cyanide concentration at $[CN^-] \geq 0.005$ M for the reaction of Co^{II}_2−Hc with cyanide at pH 8 and 25 °C.

Antiferromagnetic coupling was previously reported for Co(II) substituted *L. polyphemus* hemocyanin.[23] Here, the lower limit of the coupling constant is given as $|2J| > 50$ cm^{-1}. Since the optical spectrum of the *L. polyphemus* protein also shows marked differences compared to that of *C. maenas*, for Co^{II}_2−Hc it is suggested that the coordination sphere of the metal ions bound at the active site of the two proteins may not be identical. The heterogeneity in the subunit composition of *L. polyphemus* hemocyanin may contribute in complicating the overall spectroscopic properties of the protein if one assumes that the heterogeneity in polypeptide chain structure is also reflected to some extent at the active site level.[36]

The calculated *g*-values (see Table 1) are in the typical range for tetrahedrally coordinated Co(II) complexes, varying from 2.2 to 2.5.[33] As shown in Figures 1 and 2 for Co^{II}_2−Hc, the magnetic moment, expressed per Co(II) atom, of 2.56 μ_B at room temperature decreases to a value of 1.29 μ_B at 4.2 K. This is due to zero field splitting effects, which are characteristically observed for Co(II) complexes.[37] However, no attempt was made to include the zero field splitting parameter *D* in the calculation of the limit exchange integral as a responsible effect for the magnetic behavior. Tetrahedral Co(II) complexes are known to show small values of $D < 13$ cm^{-1},[39] and for this $2J \gg 2D$.

A similar feature is found for Co^{II}_2−N_3−Hc: here, the magnetic moment decreases from 1.98 μ_B at 182 K to 1.49 μ_B at 4.2 K. The presence of zero field splitting is reflected in the Θ-values, which are found to be −5.0 and −1.56 K, respectively, and therefore are in the range characteristically observed for Co(II) complexes.[37] It should be mentioned again that, due to the high scattering of the experimental data, the fitting parameters may vary and, hence, are not significantly different. For this reason a detailed discussion regarding the parameters *P* and TIP will be omitted. It should be pointed out that small variations in the parameters *g*, Θ, *P*, and TIP do not influence the given limits of the exchange coupling constants.

Comparing Co^{II}_2−Hc and Co^{II}_2−N_3−Hc, it follows that the exchange of the bridging ligand does not markedly influence the strength of the antiferromagnetic coupling. Hence, it may be postulated that the metal−metal distance does not change significantly upon substitution of the external ligand. This result is supported by EXAFS measurements, from which equivalent Co−Co distances are obtained for both Co^{II}_2−Hc and Co^{II}_2−N_3−Hc.[53] Furthermore Co^{II}_2−N_3−Hc can be considered as a model compound of azide−methemocyanin, met−N_3−Hc, a dicopper(II) Hc derivative with azide as a bridging ligand, which exhibits properties similar to oxy-Hc.

Detailed studies of dibridged Cu(II) inorganic model compounds for met−N_3−Hc with an azide bridge and a second alkoxide, hydroxo, or phenolate bridge suggested a μ-1,3-bridging mode of azide binding in the protein.[40−42] The model compound $[Cu_2(L-Et)(N_3)]^{2+}$ [40,41] and $[Cu(HB(3,5\text{-}iPr_2pz)_3)]_2(OH)(N_3)$ reproduced the spectroscopic and magnetic properties of met−N_3−Hc reasonably well. Like the protein, the model compound is diamagnetic, indicating strong antiferromagnetic coupling.[40,42] However, the strong antiferromagnetic coupling in the model compound was believed to arise from a pathway predominantly provided by the hydroxo bridge.[42] For this reason, two bridging ligands were postulated in met−N_3−Hc.[41,42] Since the presence of an endogenous bridging ligand could be ruled out by the X-ray structure of hemocyanin,[14,15,19] an exogenous ligand like hydroxide was assumed to represent the second bridge.[40] However, up to now no appropriate monoazido model compound was available to show whether an azide bridge alone could mediate such strong antiferromagnetic coupling.

Studies on inorganic model compounds have shown that the strength of antiferromagnetic coupling in dinuclear metal sites can be correlated to the spin of the metal ions. Metal substitution in the direction of Cu(II) → Ni(II) → Co(II) → Fe(II) leads to reduced antiferromagnetic coupling.[43] Hence, it follows that even stronger antiferromagnetic coupling is expected for the dicopper(II) derivative met−N_3−Hc than that observed for Co^{II}_2−N_3−Hc. To our knowledge, Co^{II}_2−N_3−Hc is the only

(36) Topham, R. W.; Tesh, S.; Bonaventura, C.; Bonaventura, J. In *Invertebrate Dioxygen Carriers*; Linzen, B., Ed.; Springer Verlag: Berlin, 1986; pp 407−416.
(37) Casey, A. T.; Mitra, S. In *Theory and Applications of Molecular Paramagnetism*; Boudreaux, E. A., Mulay, L. N., Eds.; John Wiley & Sons: New York, 1976; pp 135−256.
(38) Kaden, T. A.; Holmquist, B.; Vallee, B. L. *Biochem. Biophys. Res. Commun.* **1972**, *46*, 1654−1661.
(39) Makinen, M. W.; Yim, M. B. *Proc. Natl. Acad. Sci. USA* **1981**, *78*, 6221−6225.
(40) Pate, J. E.; Ross, P. K.; Thamann, T. J.; Reed, C. A.; Karlin, K. D.; Sorrell, T. N.; Solomon, E. I. *J. Am. Chem. Soc.* **1989**, *111*, 5198−5209.
(41) Reed, C. A.; Orosz, R. D. In *Research Frontiers in Bioinorganic Chemistry*; O'Connor, C. I., Ed.; World Scientific Publishing Co. Pte. Ltd.: Singapore, 1993; pp 351−415.
(42) Kitajima, N.; Fujisawa, K.; Hikichi, S.; Moro-oka, Y. *J. Am. Chem. Soc.* **1993**, *115*, 7874−7875.
(43) Lambert, S. L.; Hendrickson, D. N. *Inorg. Chem.* **1979**, *18*, 2683−2686.

Table 4. Rate Constants k_{obsd} and Amplitudes ΔA for the Reaction of Co^{II}_2−Hc (8.79×10^{-5} M) with Cyanide at pH 8 and 25 °C, Obtained upon Fitting of the Absorbance/Time Data at 560 nm to Equation 7

	step 1		step 2		step 3	
$[CN^-]$/(mol/L)	$k_{obsd.1}/s^{-1}$	$-\Delta A_1/10^{-2}$	$k_{obsd.2}/(10^{-2}\ s^{-1})$	$\Delta A_2/10^{-2}$	$k_{obsd.3}/(10^{-4}\ s^{-1})$	$\Delta A_3/10^{-2}$
0.0005	6.3 ± 1	4.16 ± 0.4	4.4 ± 0.7	0.61 ± 0.05		
0.001	2.2 ± 0.24	5.33 ± 0.57	4.3 ± 0.46	1.46 ± 0.1		
0.005	69.0 ± 6.2	7.73 ± 0.54	1.4 ± 0.15	1.2 ± 0.15	0.38 ± 0.02	2.4 ± 0.3
0.01	92.8 ± 7.5	7.56 ± 0.53	1.6 ± 0.19	1.67 ± 0.12	1.25 ± 0.15	2.5 ± 0.3
0.05	191.5 ± 15.3	7.44 ± 0.6	2.7 ± 0.16	2.57 ± 0.23	25.4 ± 1.27	8.4 ± 1.3
0.1	222.9 ± 20	8.36 ± 0.75	3.0 ± 0.21	3.63 ± 0.3	41.8 ± 3.8	5.9 ± 0.7

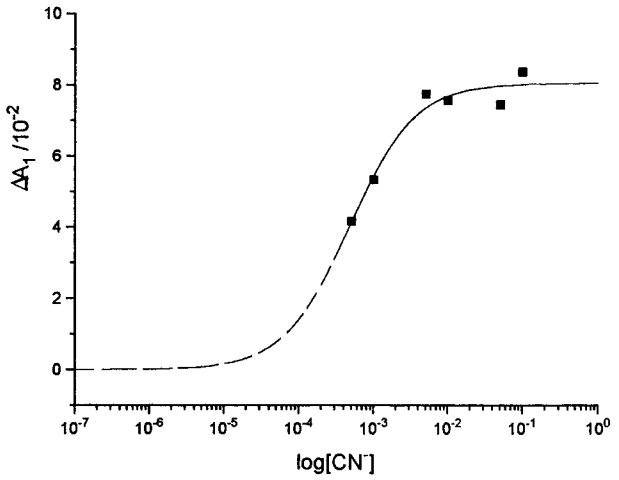

Figure 11. Plot of the dependence of the amplitude ΔA_1 on cyanide concentration according to relationship 15 (the solid line is based on the parameters $K_1 = 2100 \pm 400\ M^{-1}$ and $A_{ad} - A_0 = (8.0 \pm 0.2) \times 10^{-2}$. The broken line indicates the part of the curvature where no experimental data points are available.

example which shows that a monoazide bridge alone can mediate strong antiferromagnetic coupling. Thus, the possibility that only a single bridging ligand is present in met−N_3−Hc might not be ruled out completely. Furthermore it should be mentioned that from the presented data it cannot be concluded whether azide bridges in a μ-1,3 or in a μ-1,1 binding mode.

Co(II)−Hc. As shown in Figure 3 the magnetic moment of Co^{II}−Hc shows strong variation with temperature. It continuously decreases from 3.38 μ_B at room temperature until a plateau is reached of 2.11 μ_B at 60 K and, finally, 1.38 μ_B at 4.2 K. The strong decrease at low temperatures is probably due to zero field splitting, again reflected in the Weiss constant ($\Theta = -10.4$ K). The strong variation of the magnetic moment with temperature in the high-temperature range clearly indicates the presence of impurities of a coupled metal site. A good fit was obtained by applying eq 2, from which the amount of coupled Co^{II}_2, $S_1 = S_2 = {}^3/_2$ centers was calculated to be about 12%. The value of the exchange constant of that dinuclear impurity was calculated as $J = -191\ cm^{-1}$, which is within the range of the estimated lower limit of the antiferromagnetic exchange coupling of $|J| > 100\ cm^{-1}$ found for Co^{II}_2−Hc.

The *g*-value is in the typical range for tetrahedrally coordinated Co(II) complexes, while the magnetic moment per Co(II) is smaller as compared to those of low-molecular weight inorganic compounds, typically in the range 4.59 μ_B for $CoCl_4^{2-}$ and 4.77 μ_B for CoI_4^{2-}.[33] This discrepancy can be explained as being due to distortions from the tetrahedral coordination geometry within the mononuclear derivative, which leads to a reduced magnetic moment.[37] Another possible reason for the discrepancy may be due to an error in the applied diamagnetic correction, which is reflected in the calculation of the magnetic moment. However, this effect is compensated for by the TIP parameter and does not effect the other fitting parameters. Finally it should be pointed out, that although the magnetic behavior of Co^{II}_2−Hc, Co^{II}_2−N_3−Hc, and Co^{II}−Hc points to a tetrahedral geometry, possibility of a square pyramidal five coordination geometry cannot be totally ruled out from the magnetic susceptibility measurements alone. Hence, MCD experiments were performed. However, a square pyramidal coordination geometry is generally observed for Co(II) low-spin complexes, while high-spin Co(II) is present in all investigated Hc derivatives, as demonstrated in this work.

Magnetization Measurements. From optical spectroscopic investigations it could not be concluded, whether the active site geometry of Co^{II}−Hc was a distorted tetrahedral or a mixture of tetrahedral and square planar coordination geometry.[22] The EPR spectrum, although characteristic of high-spin Co(II), cannot be used to unambigiously assign an unique set of *g*-values to a single rhombic or axial species.[22] Furthermore the absorptivity per Co(II) of $\epsilon \sim 300\ M^{-1}\ cm^{-1}$ is much smaller as compared to $\epsilon \sim 450\ M^{-1}\ cm^{-1}$ per Co(II) for the dinuclear derivative. It is suggested that the mononuclear derivative might thus be a mixture.

The experimental data shown in Figure 4 are in good agreement with the theoretical curvature expected for a $S = {}^3/_2$ ion. This shows that the Co(II) in the active site of Co^{II}−Hc is in the high-spin state. Since octahedrally coordinated Co(II), showing $\epsilon \sim 10\ M^{-1}\ cm^{-1}$, can be ruled out due to the absorptivity per Co(II) of $\epsilon \sim 300\ M^{-1}\ cm^{-1}$ in the protein, it can be concluded that the near-tetrahedral coordination geometry is unambiguously retained in the mononuclear Co^{II}−Hc derivative.

Magnetic Circular Dichroism Spectroscopy. The analysis and structural interpretation of the MCD spectra are largely qualitative, since Co(II) compounds show complex spectra. The assignment of the observed bands to the corresponding electronic transitions is not straightforward. A comparison of small-molecule Co(II) spectra, which exemplify typical MCD spectra of octahedral, pentacoordinate, and tetrahedral coordination geometries,[38] reveal that the spectra of tetrahedrally coordinated complexes are closely comparable to those of the Co(II) substituted hemocyanin derivatives under investigation. Moreover, the MCD spectra bear striking similarities to the spectra of other Co(II) substituted metalloproteins, such as carbonic anhydrase at high pH,[44] carboxypeptidase A, procarboxypeptidase A, and thermolysin[45] as well as insulin.[46,47] Detailed electronic absorption, MCD, and CD studies on cobalt(II)−carbonic anhydrase together with comparisons with spectra of well-characterized inorganic Co(II) complexes indicate that the spectrum of cobalt(II)−carbonic anhydrase arises from a trigonally distorted tetrahedral Co(II) geometry.[44]

The absorption and MCD bands of the Co(II) chromophore are attributed to the ν_3 transition ${}^4A_2 \rightarrow {}^4T_1(P)$[21,34]

(44) Coleman, J. E.; Coleman, R. V. *J. Biol. Chem.* **1972**, *247*, 4718−4728.
(45) Holmquist, B.; Kaden, T. A.; Vallee, B. L. *Biochemistry* **1975**, *14*, 1454−1460.
(46) Roy, M.; Brader, M. L.; Lee, R. W.-K.; Kaarsholm, N. C.; Hansen, J. F.; Dunn, M. F. *J. Biol. Chem.* **1989**, *264*, 19081−19085.
(47) Brader, M. L.; Kaarsholm, N. L.; Lee, R. W.-K.; Dunn, M. F. *Biochemistry* **1991**, *30*, 6636−6645.

Moreover, the spectra of Co(II) substituted hexameric insulin,[47] Co(II) substituted *L. polyphemus* hemocyanin at high pH,[27] and *Sepioteuthis lessonia* (*S. lessonia*) hemocyanin[20] have a band pattern indicative of a distorted tetrahedral Co(II) structure. The MCD spectra of the Co(II) substituted derivatives of *C. maenas* Hc are also closely comparable to those of Co(II) substituted *L. polyphemus* Hc at high pH and of Co(II) substituted *S. lessonia* Hc, indicating a related coordination sphere of the Co(II) substituted metal site.

From near-infrared MCD studies, further indication of a tetrahedral coordination sphere is obtained. The ν_2 electronic transitions are difficult to observe in absorption spectroscopy, not only due to their low intensities but also due to the overlap with vibrational overtone bands.[48] However, vibrational bands exhibit only small MCD signals,[34] and therefore this technique allows us to observe these electronic transitions with greater sensitivity.

Visible and near-infrared MCD spectra were reported for the Co(II) substituted blue copper proteins azurin, plastocyanin, and stellacyanin.[34] The observed band pattern in the near-infrared region was assigned to C terms of opposite signs (pseudo-A terms), which result from spin−orbit coupling in the spin-allowed ν_2 transition $^4A_2 \rightarrow {}^4T_1(F)$ in a tetrahedral d^7 complex.[48] The high degree of similarity between the visible and near-infrared MCD spectra discussed above and those of Co^{II}_2−Hc and Co^{II}_2−N_3−Hc allow us to assign the coordination geometry around the Co(II) center as close to tetrahedral. The band patterns in the near-infrared are consistent with C terms of opposite sign; the splitting can be associated with spin−orbit coupling.[34] Also the low-temperature MCD spectrum of Co^{II}_2−Hc is in agreement with a tetrahedral structure since the characteristic band pattern is preserved. In comparison to the room temperature MCD spectrum, the low-temperature spectrum shows a large increase in intensity by a factor of ca. 4, which characteristically arises from C terms.[49]

Furthermore, the addition of small anions, like chloride, cyanide, and azide, results in increased absorptivity for Co(II) as well as in distinct changes in the band positions of absorption spectra for Co^{II}−Hc [22] and Co^{II}_2−Hc.[54] These changes are attributed to the addition of the respective anions to Co(II) while also maintaining the overall tetrahedral coordination geometry of the metal ion. This assignment was made from the observed intense spectra where $\epsilon > 300\ M^{-1}\ cm^{-1}$, which is characteristic for tetrahedral Co(II) complexes, while octahedral complexes give rise to broad spectra with low intensity ($\epsilon \sim 10\ M^{-1}\ cm^{-1}$) and pentacoordinate Co(II) complexes display spectra with intensities where $100 < \epsilon < 300\ M^{-1}\ cm^{-1}$.[48] However, the interpretation of the Co(II) protein spectra is not straightforward because differentiation in UV/vis spectra between tetrahedral spectra and pentacoordinate geometry is often unclear.[48] Further, the introduced ligand may either substitute a present bridging ligand, maintaining a tetracoordinate geometry, or be added as a further bridging ligand, establishing a pentacoordinate metal site. Ligand binding to one metal center would also result in a pentacoordination geometry. However, tetrahedral and pentacoordinated Co(II) complexes can be clearly distinguished by MCD spectroscopy, since both species show characteristic MCD spectra, exhibiting much different band shapes.[45] Since results of our MCD studies establish the tetrahedral coordination geometry of Co^{II}_2−N_3−Hc, it can be concluded that the addition of azide to the tetrahedral complex Co^{II}_2−Hc leads to a ligand exchange and not to the addition of the anion. Otherwise a pentacoordinate species would have been observed. Since after addition of small ions like chloride or cyanide to Co^{II}_2−Hc the UV/vis spectra of these products display absorptivities which are closely comparable to those of Co^{II}_2−N_3−Hc, it is reasonable to assume tetrahedral coordination geometry for these complexes as well. Consequently the reaction of Co^{II}_2−Hc with small anions can be attributed to a ligand exchange reaction.

Furthermore our variable temperature magnetic susceptibility measurements have shown strong antiferromagnetic exchange coupling between the metal centers in Co^{II}_2−Hc as well as in Co^{II}_2−N_3−Hc. Previously it was demonstrated that the strong antiferromagnetic coupling necessitates the existence of a bridging ligand. Since it could be established that the Co(II) ions in Co^{II}_2−N_3−Hc exhibit tetracoordination geometry and considering the fact that Co^{II}_2−N_3−Hc is prepared from Co^{II}_2−Hc by addition of azide, it can be concluded that an exchange of the bridging ligand must have taken place. Thus, an additional conceivable model can now be excluded, in which the loss of a bridging ligand in favor of the ligation of the introduced anion leads again to two four-coordinated but nonbridged metal ions, revealing also tetrahedral coordination geometry.

Further support for tetrahedral coordination geometry of the Co(II) substituted Hc derivatives was achieved from ligand field calculations. The strength of the ligand field Δ_t was evaluated from the approximate term energies of the ν_2- and ν_3-transitions. Hence, a value of $\Delta_t = 5000 \pm 300\ cm^{-1}$ followed. Within the experimental error it is not possible to differentiate between the Δ_t-values of the various Co(II) substituted derivatives studied. The calculated value is comparable to the strength of the tetrahedral ligand field $\Delta_t = 5100 \pm 300\ cm^{-1}$ found for Co(II) substituted *L. polyphemus* Hc[23] and Co(II) complexes of low molecular weight ($\Delta_t \sim 5000\ cm^{-1}$), which are mainly coordinated by nitrogen ligands.[50] Slightly lower values were determined for Co(II) substituted blue copper proteins ($\Delta_t = 4900\ cm^{-1}$)[34] and metallothionein ($\Delta_t = 4780\ cm^{-1}$),[51] which reflect the influence of the weak ligand field nature of the sulfur ligands. Thus, ligand field analysis substantiates a tetrahedral structure as suggested previously.

In contrast to the dinuclear Co^{II}_2−Hc derivatives, the MCD spectrum of the mononuclear Co^{II}−Hc derivative suggests distortions from the basic tetrahedral coordination of the Co(II) ion. A broadened half-bandwidth is clearly observed as compared to that of the dinuclear derivatives. Furthermore the value of $\Delta\epsilon/B$ per Co(II) atom is considerably smaller (by a factor of ca. 2.5) than those of the dinuclear derivatives. This effect is also reflected in reduced optical absorptivities. Here, the absorptivities per Co(II) differ by a factor of ca. 1.5 ($\epsilon(Co^{II}_2\text{−Hc}) = 450\ M^{-1}\ cm^{-1}$; $\epsilon(Co^{II}\text{−Hc}) \sim 300\ M^{-1}\ cm^{-1}$).[28] It was suggested, that the difference is due to the presence of a second metal ion at the active site.[28]

The spectrum of the mononuclear Co^{II}−Hc derivative is shifted toward higher energies with respect to the derivatives containing two metal ions in the active site (Table 2). The variation of the MCD band position is presumably due to minor differences in the energy levels of the Co(II) chromophore, which on the other hand may reflect alterations of the ligand field strength and spin−orbit coupling. Different Weiss constants Θ, which here reflect spin−orbit coupling, were obtained from our magnetic susceptibility studies and support this suggestion.

The near-infrared MCD spectrum of Co^{II}−Hc is closely comparable to the spectra of the dinuclear derivatives and to

(48) Lever, A. B. P. *Inorganic Electronic Spectroscopy*; Elsevier: Amsterdam, 1984.
(49) Schatz, P. N.; Mc Caffery, A. *J. Q. Rev.* **1969**, *23*, 552−584.
(50) Rosenberg, R. C.; Root, C. A.; Gray, H. B. *J. Am. Chem. Soc.* **1975**, *97*, 21−26.
(51) Vasak, M.; Kägi, J. H. R.; Holmquist, B.; Vallee, B. L. *Biochemistry* **1981**, *20*, 6659−6664.

those of Co(II) substituted blue copper proteins and is hence also indicative of a tetrahedral structure. As already discussed for the dinuclear derivatives, the band pattern is consistent with a C term of opposite sign and the calculated strength of the ligand field is comparable to the values observed for other tetrahedrally coordinated Co(II) complexes.[34,50,51]

Considering the fact that MCD arises from the splitting of energy levels induced by an external magnetic field, it can be summarized that a similar set of basic energy levels and hence a similar coordination geometry exists for the dinuclear Co(II) substituted derivatives Co^{II}_2−Hc and Co^{II}_2−N_3−Hc, which is close to tetrahedral, while the mononuclear Co^{II}−Hc shows displacements to a less tetrahedral Co(II) geometry.

Assertions regarding the ability of Co(II) substituted hemocyanins to bind dioxygen are controversial. While Dutton et al.[24] and Larrabee et al.[27] report the formation of oxygenated Co substituted *L. polyphemus* hemocyanin on the basis of CD and MCD measurements, dioxygen binding could not be substantiated by others.[21,23] Also, for Co(II) substituted *C. maenas* hemocyanin no evidence for oxygen binding could be found.[28] For the *L. polyphemus* study,[27] care was not taken to remove adventitiously bound Co(II), which could explain the effects observed.

Dioxygen binding would be accompanied by the formal oxidation of Co(II), leading to a dinuclear Co(III) metal site showing octahedral coordination geometry. In analogy with oxy-Hc, the structure could be formulated as Co^{III}−O_2−Co^{III}. In contrast to tetrahedrally coordinated Co(II), octahedrally coordinated Co(III) gives rise to a very weak MCD signal, characterized by a slightly structured, negative MCD band centered near 510 nm.[45] For this reason MCD spectra for octahedral Co(III) are clearly distinguishable from those of Co(II) in tetrahedral coordination geometry.[44] Since in the presence of dioxygen an intense MCD signal is observed for Co^{II}_2−Hc, which is typical for Co(II) in tetrahedral coordination geometry, it can be concluded that the formation of a Co^{III}−O_2−Co^{III} complex does not occur. Hence, it follows that the Co^{II}_2−Hc derivative of *C. maenas* Hc is not oxygenated under the experimental conditions given.

Kinetics of the Reaction of $Co(II)_2$−Hc with Cyanide. Within the group of ligands capable of binding to the metal site of Co(II) substituted hemocyanin, cyanide is particularly interesting because it can both coordinate and remove the metal[22,28] in the form of cyano complexes. It is not surprising, therefore, that the overall reaction of Co^{II}_2−Hc with cyanide is a three-step process consisting of an initial cyanide addition reaction and subsequent slow biphasic cobalt removal.

The initial addition of cyanide according to (9) is thermodynamically favored with K_1 estimated to be 2100 ± 400 M^{-1}.

$$Co^{II}_2\text{−Hc} + CN^- \overset{K_1}{\rightleftharpoons} \text{adduct} \qquad (9)$$

The kinetics of cyanide addition are such that outer sphere complexation according to (12) precedes cyanide coordination according to (13). Taking the size of $K_{os} = 62 \pm 8$ M^{-1} as a measure for electrostatically controlled ion pairing, one has to conclude that the cyanide anion interacts with a substrate of high positive overall charge (for an ionic strength of 0.1 M theory would predict $K_{os} = 35$ M^{-1} for a −1/+5 charge type interaction and $K_{os} = 89$ M^{-1} for a −1/+6 interaction.[52] The present data do not allow any reliable conclusion concerning the chemical nature of the outer sphere complex $\{Co^{II}_2\text{−Hc}, CN^-\}$. From the kinetic data no information about the binding of CN^- can be obtained. The cyanide ion could well be electrostatically attached to the cobalt site but attachment to any other positively charged domain of the protein cannot be excluded. A detailed discussion of the rate of cyanide coordination according to (13) with $k_{ad} = 256 \pm 10$ s^{-1} is therefore not very meaningful.

$$Co^{II}_2\text{−Hc} + CN^- \overset{K_{os}}{\rightleftharpoons} \{Co^{II}_2\text{−Hc}, CN^-\} \qquad (12)$$

$$\{Co^{II}_2\text{−Hc}, CN^-\} \xrightarrow{k_{ad}} \text{adduct} \qquad (13)$$

The biphasic cobalt removal following cyanide addition is comparatively slow. The dependence $k_{obsd.2} = f([CN^{-1}])$ is also of the saturation type (see eqs 12 and 13), whereas $k_{obsd.3}$ appears to increase linearly with $[CN^-]$. One can speculate as to whether species such as $[Co(CN)_5]^{3-}$ are involved as intermediates. Since dioxygen is present, it is reasonable to assume that, at high cyanide concentrations, the final product is the species $[Co(CN)_6]^{3-}$.

Conclusions

To summarize, strong antiferromagnetic coupling was found for Co^{II}_2−Hc and Co^{II}_2−N_3−Hc, providing evidence for the presence of a bridging ligand in the Co(II) substituted active site. Together with MCD measurements, showing that each Co(II) in the dinuclear Co(II) substituted derivatives under investigation is tetracoordinate, it is concluded that addition of small anions like azide leads to substitution of a putative bridging ligand. Since azide mediates strong antiferromagnetic coupling and represents the only bridging ligand in Co^{II}_2−N_3−Hc, which is a model compound for azide−methemocyanin, the possibility of a single bridging ligand in the latter is supported.

Furthermore no evidence for an octahedrally coordinated Co(III) species could be obtained from magnetic or magnetooptical studies, implying that the oxidation of Co(II) to Co(III) and hence the formation of an oxygenated Co^{III}−O_2−Co^{III} Hc derivative does not occur.

A comparison of the MCD spectra of the dinuclear and the mononuclear Co(II) substituted derivatives shows that the coordination geometry is also influenced by the neighboring metal ion. This result supports corresponding observations from UV/vis spectra. A less tetrahedral coordination geometry seems to be achieved if only one metal ion is present in the binuclear active site. In spite of the observed spectral changes Co(II) remains in the high-spin form in Co^{II}−Hc, as shown by magnetization studies.

The reaction of Co^{II}_2−Hc with cyanide is a three-step process. The initial step consists in a fast cyanide addition reaction, leading to an adduct, the formation of which is thermodynamically favored. The formation of the adduct, which may be preceded by outer-sphere association of the cyanide, is followed by slow, cyanide-assisted cobalt removal in two steps.

Once more it is shown that, in metalloproteins, metal substitution provides an effective method for describing structural parameters of the active site.

Acknowledgment. W.H., M.H., and H.E. thank the Deutsche Forschungsgemeinschaft for financial support. H.E. also thanks the Verband der Chemischen Industrie e.V. J.P. acknowledges support by N.I.H. Grants GM-40168 and RR-02583.

IC951587Z

(52) Jordan, R. B. *Reaction Mechanisms of Inorganic and Organometallic Systems*; Oxford University Press: Oxford, U.K., 1991.
(53) Bubacco, L. Manuscript in preparation.
(54) Hüber, M.; Bubacco, L. Unpublished results.